

CounterNet: End-to-End Training of Counterfactual Aware Predictions

Hangzhi Guo¹, Thanh Hong Nguyen², and Amulya Yadav¹

¹*College of Information Sciences and Technology, Pennsylvania State University*

²*Computer and Information Science, University of Oregon*

Abstract

This work presents *CounterNet*, a novel *end-to-end* learning framework which integrates the predictive model training and counterfactual (CF) explanation generation into a single end-to-end pipeline. Counterfactual explanations attempt to find the smallest modification to the feature values of an instance that changes the prediction of the ML model to a predefined output. Prior CF explanation techniques rely on solving separate time-intensive optimization problems for every single input instance to find CF examples, and also suffer from the misalignment of objectives between model predictions and explanations, which leads to significant shortcomings in the quality of CF explanations. CounterNet, on the other hand, integrates both prediction and explanation in the same framework, which enables the optimization of the CF example generation only *once* together with the predictive model. We propose a novel variant of back-propagation which can help in effectively training CounterNet’s network. Finally, we conduct extensive experiments on multiple real-world datasets. Our results show that CounterNet generates high-quality predictions, and corresponding CF examples (with high validity) for any new input instance significantly faster than existing state-of-the-art baselines.

1 Introduction

Most prior work in Explainable Artificial Intelligence (XAI) has been focused on developing techniques to interpret decisions made by black-box ML models. For example, widely known approaches rely on attribution-based explanation for interpreting an ML model (e.g., LIME (Ribeiro et al., 2016) and SHAP (Lundberg and Lee, 2017)). These approaches can help computer scientists understand why (and how) ML models make certain predictions. However, end users (who generally have no ML expertise) are often more interested in understanding actionable implications of the ML model’s predictions (as it relates to them), rather than just understanding how these models arrive at their predictions. For example, if a person applies for a loan and gets rejected by a bank’s ML algorithm, he/she might be more interested in knowing what they need to change in a future loan application to successfully get a loan, rather than understanding how the ML system makes all of its decisions.

Thus, from an end-user perspective, counterfactual (CF) explanation techniques¹ (Wachter et al., 2017) may be more preferable. A CF explanation offers a contrastive case — to explain the predictions made by an ML model on data point x , CF explanation methods find a new *counterfactual* point x' , which is close to x but gets a different (or opposite) prediction from the ML model. CF explanations are useful because they can also be used to offer recourse to vulnerable groups. For example, when an ML model spots a student as

¹Counterfactual explanation is also closely related to algorithmic recourse (Ustun et al., 2019) and contrastive explanation (Dhurandhar et al., 2018). Although these terms are proposed under different contexts, their differences to CF explanation has been blurred (Verma et al., 2020), i.e. these terms are used interchangeably. Further, the literature on counterfactual explanations is unrelated to “counterfactuals” in causal inference.

being vulnerable to dropping out from school, CF explanation techniques can suggest corrective measures to teachers, who can intervene accordingly.

Unfortunately, existing CF explanation techniques suffer from two major limitations: First, existing techniques are post-hoc in nature and are mainly designed to interpret proprietary models (see discussions in Section 6), i.e., they assume a trained black-box ML model as input. As a result, the training procedure of this ML model is completely uninformed by the optimization procedure that finds CF examples in existing techniques. Unfortunately, this procedure causes the generated CF to align poorly with the original black-box model, causing shortcomings in the validity of the generated CF examples (we illustrate this in Section 5). Furthermore, most prior techniques search for CF examples by solving a separate optimization problem for each input instance (Wachter et al., 2017; Mothilal et al., 2020; Ustun et al., 2019). This optimization problem is computationally intensive and it requires an excessive amount of time, which is not viable in time-constrained environments, e.g., runtime is an important consideration if CF explanation techniques are deployed in end-user facing devices such as smartphones, etc.

In this paper, we propose *CounterNet*, a novel learning framework that combines the training of the ML predictive model and the generation of corresponding CF examples into a single end-to-end (i.e., from input to prediction to explanation) pipeline. CounterNet addresses the limitations of existing CF techniques via four key contributions. First, unlike post-hoc approaches (where CF explanations are generated after the ML model was trained), CounterNet uses a (neural network) model-based CF generation method, enabling the joint training of its CF generation network and the predictor network. This joint training is key to better alignment between CF explanation and prediction, which leads to superior performance (as we show in Section 5). Second, to overcome challenges in effectively training CounterNet, we propose a new loss function formulation, a new variant of back-propagation procedure, and use label smoothing techniques to stabilize CounterNet’s network training process. By adopting this end-to-end learning process, CounterNet can generate CF examples with high validity and proximity while ensuring that its predictor network also produces highly accurate predictions. Third, we introduce the *insensitivity score* as an important metric to evaluate the real-world usability of CF explanation techniques, which stems from a desire to present explanations to end-users in terms of fewer feature differences (between the input and the CF example).

Finally, we conduct a rigorous experimental evaluation of CounterNet on six datasets. Our analysis shows that CounterNet outperforms state-of-the-art CF explanation techniques. It is the only method that consistently achieves more than 98% validity (which ensures that CF examples are valid, i.e., they get opposite predictions from the ML model) and 94% insensitivity score (which ensures that the CF examples remain valid after ignoring small differences between the input and the CF example). Additionally, CF examples generated by CounterNet are highly proximal (i.e., the L_1 norm distance between the input instance and the CF example is small) as compared to baseline techniques. Finally, CounterNet runs orders of magnitude faster than state-of-the-art baselines.

2 Related Work

Broadly, to ensure that models’ predictions are interpretable to end-users, two distinct approaches have been proposed in prior work: (i) applying “glass-box” ML models (e.g., decision trees, rule lists, etc.) that are intrinsically interpretable (Rudin, 2019; Lou et al., 2013; Caruana et al., 2015; Lakkaraju et al., 2016); and (ii) applying “black-box” ML models, and explaining their predictions in a post-hoc manner (Ribeiro et al., 2016; Chen et al., 2019; Wachter et al., 2017). We focus on the black-box ML model approach, as interpretable models often come at the cost of decreased predictive accuracy (Agarwal, 2020), which limits the usability of these methods.

Several explanation techniques for black-box ML models exist: (i) Ribeiro et al. (2016) propose a method called LIME, which generates local explanations by sampling data near the input instance and uses a linear model to fit this data. (ii) Lundberg and Lee (2017) introduce SHAP, a unified explanation framework to find locally faithful explanations by using the Shapley value concept in game theory. However, these methods are of limited utility to average end-users, who are often more interested in understanding actionable implications of these ML model predictions (as it relates to them), rather than understanding decision rules used by ML models to make predictions.

Our work is closely related to prior literature on counterfactual explanation techniques, which finds new instances that lead to different predicted outcomes. Wachter et al. (2017) propose *VanillaCF* which generates CF examples by minimizing the distance between the input instance and the CF example, while pushing the new prediction towards the desired class. (e.g., pushing the model’s prediction from getting rejected to getting approved, in an ML based loan approval/rejection domain). Other algorithms, built on top of *VanillaCF*, optimize other aspects, such as recourse cost (Ustun et al., 2019), fairness (Sharma et al., 2020), diversity (Mothilal et al., 2020), closeness to the data manifold (Van Looveren and Klaise, 2019; Pawelczyk et al., 2020), and causal constraints (Karimi et al., 2021). Previous studies (Binns et al., 2018; Bhatt et al., 2020) show that counterfactual explanations benefit end-users to make decisions. Unfortunately, most prior work follows a post-hoc approach (explaining model’s output after a trained ML model is provided). This post-hoc approach is not only time-consuming, but is also exposed to the issue of misalignment between the predictive model training and the counterfactual example generation (as we show in Section 5). In our work, we propose CounterNet, an end-to-end framework which overcomes these limitations to efficiently generate accurate predictions, and corresponding highly-aligned CF explanations.

3 The Proposed Framework: CounterNet

Unlike prior work, our proposed framework CounterNet relies on a novel integrated architecture which combines the predictive model training and the counterfactual example generation into a single optimization framework. This integration allows us to optimize the CF example generation component only once together with the predictive model training component (as part of a single neural network architecture). Through this integration, we can simultaneously optimize the accuracy of the trained predictive model and the quality of the generated counterfactual examples. Moreover, the model prediction and the CF example generation both derive from a shared component. This design leads to closer alignment between prediction and explanation.

Formally, given an input instance $x \in \mathbb{R}^d$, CounterNet aims to generate two outputs: (i) the ML prediction component outputs a prediction \hat{y}_x for input instance x ; and (ii) the CF example generation component produces a CF example $x' \in \mathbb{R}^d$ as an explanation for input instance x . Ideally, the CF example x' should get a different (and often more preferable) prediction $\hat{y}_{x'}$, as compared to the prediction \hat{y}_x on the original input instance x (i.e., $\hat{y}_{x'} \neq \hat{y}_x$). In particular, if the desired prediction output is binary-valued, then \hat{y}_x and $\hat{y}_{x'}$ should take on opposite values (i.e., $\hat{y}_x + \hat{y}_{x'} = 1$).

3.1 Network Architecture

Figure 1 illustrates CounterNet’s architecture which includes three components: (i) an encoder network $h(\cdot)$; (ii) a predictor network $f(\cdot)$; and (iii) a CF generator network $g(\cdot)$. During training, each input instance $x \in \mathbb{R}^d$ is first passed through the encoder network to generate a dense latent vector representation of x (denoted by $z_x = h(x)$). Then, this latent representation is passed through both the predictor network and the CF generator network. The predictor network outputs a softmax representation of the prediction $\hat{y}_x = f(z_x)$. To generate CF explanation, the CF generator network takes two pieces of information: (i) the final representation of the predictor network p_x (before it is passed through the softmax layer), and (ii)

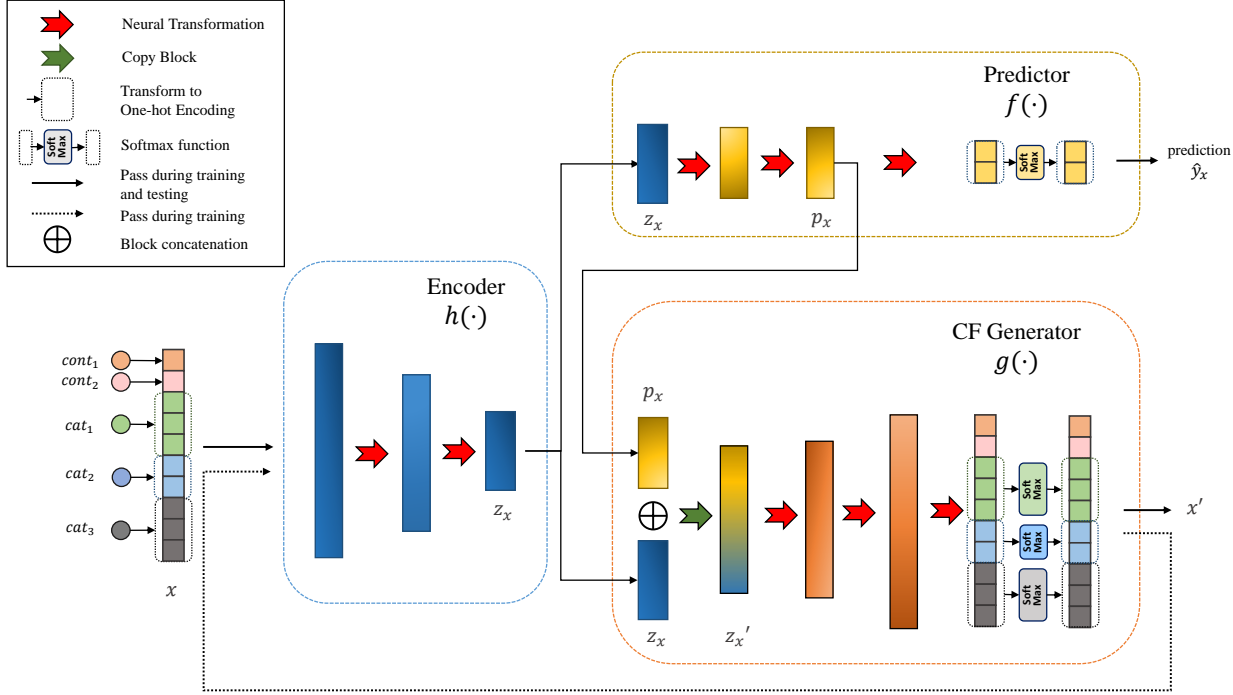


Figure 1: CounterNet contains three components: an encoder (blue) which transforms the input into a dense latent vector, a predictor network (yellow) which outputs the prediction, and a CF generator (orange) which produces explanations.

the latent vector z_x . These two vectors are concatenated as the final latent vector $z'_x = p_x \oplus z_x$, which is passed through CF generator to produce a CF example $x' = g(z'_x)$ for input instance x . Note that the predictor network’s final representation is also passed as an input to the CF generator network in order to avoid misalignment between the generated prediction and CF example.

Furthermore, to ensure that the CF generator network outputs valid CF examples (i.e., $\hat{y}_x \neq \hat{y}_{x'}$), the output of the CF generator network x' is also passed back as an input through the encoder and predictor networks when training CounterNet. This additional feedback loop (from the output of CF generator network back into the encoder and predictor networks) optimizes the *validity* of generated CF examples. That is, we can now train the entire network in a way such that the predictor network outputs opposite predictions \hat{y}_x and $\hat{y}_{x'}$ for the input instance x and the CF example output by the CF generator network x' , respectively. Note that this “*feedback loop*” neuronal connection is only needed at training time, and is removed at test time. Figure 1 shows neuronal connections required during training and test times using solid and dashed arrows, respectively.

Design of Encoder, Predictor & CF Generator. All three components in CounterNet’s architecture consist of a multi-layer perception (MLP). The encoder network in CounterNet consists of two feed-forward layers that down-sample to generate a latent vector $z \in \mathbb{R}^k$ (s.t. $k < d$). The predictor network passes this latent vector z through two feed-forward layers to produce the predictor representation p . Finally, the predictor network outputs the probability distribution over predictions with a fully-connected layer. On the other hand, the CF generator network takes the final latent representation $z' = z \oplus p$ as input, and up-samples to produce CF examples $x' \in \mathbb{R}^d$. See appendix for details on network structures.

Each feed-forward neural network layer inside CounterNet uses LeakyRelu activation functions (Xu et al., 2015) followed by a dropout layer (Srivastava et al., 2014) to avoid overfitting. Note that the MLP in the

encoder, predictor and CF generator networks can be replaced with other neuronal blocks (e.g., convolution, recurrent, attention; see Appendix for details).

Customizing for Categorical Features. To handle categorical features, we customize CounterNet’s architecture for each dataset. First, we transform all categorical features into numeric features via one-hot encoding as continuous variables between $[0, 1]$. In addition, for each categorical feature, we add a softmax layer after the final output layer in the CF generator network (Figure 1). This small adjustment ensures the generated CF examples to respect the one-hot encoding format (as the output of the softmax layer will sum up to 1). Finally, we normalize all continuous features to the $[0, 1]$ range before training.

3.2 CounterNet Loss Function

Each part of our loss function corresponds to a desirable objective in CounterNet’s output: (i) *predictive accuracy* - we expect the predictor network to output accurate predictions \hat{y}_x ; (ii) *counterfactual validity* - we expect that the CF explanation x' produced by the CF generator network are valid, i.e., they get opposite predictions from the predictor network; and (iii) *proximity* - we expect the changes from input instance x to CF explanation x' to be minimum.

Based on these characteristics, we adopt the three parts of CounterNet’s loss function as follows:

$$\begin{aligned}\mathcal{L}_1 &= \frac{1}{N} \sum_{i=1}^N (y_i - \hat{y}_{x_i})^2 \\ \mathcal{L}_2 &= \frac{1}{N} \sum_{i=1}^N (\hat{y}_{x_i} - (1 - \hat{y}_{x'_i}))^2 \\ \mathcal{L}_3 &= \frac{1}{N} \sum_{i=1}^N (x_i - x'_i)^2\end{aligned}\tag{1}$$

where N denotes the number of instances in our dataset, \mathcal{L}_1 denotes the mean squared error (MSE) between the actual and the predicted labels (y_i and \hat{y}_{x_i} on instance x_i , respectively), which aims to maximize predictive accuracy. Similarly, \mathcal{L}_2 denotes the MSE between the original predicted label on instance x_i (i.e., \hat{y}_{x_i}), and the opposite of the prediction received by the corresponding CF example x'_i (i.e., $1 - \hat{y}_{x'_i}$). Intuitively, minimizing \mathcal{L}_2 maximizes the validity of the generated CF example x'_i (for each input instance x_i) by ensuring that the predictions on x'_i and x_i are as different as possible. Finally, \mathcal{L}_3 represents the averaged distance between input instances x_i and the counterfactual examples x'_i , which aims to maximize proximity. This choice of loss functions is crucial to CounterNet’s superior performance, as replacing \mathcal{L}_1 , \mathcal{L}_2 and \mathcal{L}_3 with alternate functional forms leads to degraded performance (as we show in Section 5).

Given these three loss components, we aim to optimize the parameter θ of the overall network, which can be formulated as the following minimization problem:

$$\min_{\theta} \lambda_1 \cdot \mathcal{L}_1 + \lambda_2 \cdot \mathcal{L}_2 + \lambda_3 \cdot \mathcal{L}_3\tag{2}$$

where $(\lambda_1, \lambda_2, \lambda_3)$ are hyper-parameters to balance three loss components. Unfortunately, because of three divergent objectives, it leads to poor convergence of gradient descent for solving Eq. 2. Thus, we propose the following double-back propagation (BP) procedure to remedy this issue.

3.3 Practical Choices for Training

The conventional way of solving the optimization problem in Eq. 2 is to use gradient descent with back propagation (BP). However, as we show in Section 5, directly optimizing the objective function Eq. 2 leads to poor quality of prediction and CF explanations. This occurs because the optimization problem in Eq. 2 consists of three divergent objectives, i.e., \mathcal{L}_1 , \mathcal{L}_2 and \mathcal{L}_3 , each of which individually tries to move the

gradient in different directions. Crucially, \mathcal{L}_1 and \mathcal{L}_2 represent two different objectives (prediction and CF explanation, respectively), and as shown in Lemma 3.1, the gradients of these two objective functions move in different directions. Thus, the accumulated gradient direction (i.e., gradient across all three loss objectives at each step) fluctuates drastically, which leads to poor convergence of training.

Lemma 3.1 (Divergent Gradient Problem). *Let $\mathcal{L}_1 = \|y_i - \hat{y}_{x_i}\|^2$, and $\mathcal{L}_2 = \left\|y_i - (1 - \hat{y}_{x'_i})\right\|^2$, assuming that $x'_i \rightarrow x_i$, $0 < \hat{y}_x < 1$, and y_i is a binary label, then $\nabla_{\theta} \mathcal{L}_1 \cdot \nabla_{\theta} \mathcal{L}_2 < 0$. (See proof in Appendix)*

To remedy this issue, we propose a variant of BP. We divide the problem of optimizing Eq. 2 into two parts: (i) optimizing predictive accuracy; and (ii) optimizing the validity of CF generation. Note that in the CounterNet architecture, the predictive accuracy of the predictor network is primarily influenced by \mathcal{L}_1 , whereas the CF generation is dictated by \mathcal{L}_2 and \mathcal{L}_3 . We thus propose a double-back BP procedure to optimize these two parts. Specifically, for each mini-batch of m data points $\{x^{(i)}, y^{(i)}\}^m$, the network updates its weights θ twice through back propagation. For the first update, it computes $\theta' = \theta - \nabla_{\theta}(\lambda_1 \cdot \mathcal{L}_1)$, and for the second update, it computes $\theta'' = \theta' - \nabla_{\theta'}(\lambda_2 \cdot \mathcal{L}_2 + \lambda_3 \cdot \mathcal{L}_3)$. This procedure distributes the objective function (Eq. 2) into two stages, which lessens the difficulty in training. As we show in Section 5, this procedure leads to significantly better convergence in training as compared to the conventional BP algorithm.

Finally, inspired from Salimans et al. (2016), we also implement the label smoothing trick to further stabilize our training. Intuitively, label smoothing prevents neural networks from becoming overconfident in their predictions (Müller et al., 2019). Specifically, for each mini-batch $\{x^{(i)}, y^{(i)}\}^m$, we set each $y \sim \mathcal{U}(0.8, 0.95)$ for positive labels, and $y \sim \mathcal{U}(0.05, 0.2)$ for negative labels.

4 Experiment Setup

Baselines. We compare CounterNet against four state-of-the-art post-hoc CF explanation techniques: (i) *VanillaCF* (Wachter et al., 2017) — this method generates CF examples by optimizing proximity and CF validity; (ii) *DiverseCF* and (iii) *ProtoCF* — these two baselines generate CF examples by optimizing for diversity and consistency with prototypes, respectively; and (iv) *VAE-CF* (Mahajan et al., 2019) — this is a model-based post-hoc approach to generate CF examples. VAE-CF is the only baseline relying on a neural network model to generate CF examples, while the other three baselines generate CF examples by solving explicit optimization problems.

Unlike CounterNet, all four baselines require a trained predictive model. Thus, for each dataset, we train a neural network model and use it as the base predictive model for all baselines. For fair comparison, this base predictive model is trained as follows: (i) we discard the CF generator network inside CounterNet’s architecture (Figure 1), and only keep the encoder and predictor networks (as only these two networks are needed by CounterNet to make predictions); (ii) this combination of encoder and predictor is solely optimized for predictive accuracy (i.e., \mathcal{L}_1), and this trained model is then used as our base predictive model for all baselines. For each dataset, hyperparameter tuning was conducted separately using grid search (see Appendix for details).

Datasets. We evaluate CounterNet on six real-world binary classification datasets from diverse domains (Table 1). We remove features that contain identifiable information to protect anonymity. Our primary evaluation uses three large-sized datasets: (i) *Adult* (Kohavi and Becker, 1996) which predicts whether an individual’s income reaches \$50K using demographic data; (ii) *HELOC* (FICO, 2018) which uses financial information in credit reports to predict if a homeowner qualifies for a line of credit; and (iii) *OULAD* (Kuzilek et al., 2017) which predicts whether MOOC students drop out, based on their online learning logs.

Table 1: Summary of Datasets used for Evaluation

Dataset	Size	#Continuous	#Categorical
Adult	32,561	2	6
Student	649	2	14
Titanic	891	2	24
HELOC	10,459	21	2
OULAD	32,593	23	8
Breast Cancer	569	30	0

In addition, we experiment with three small-sized datasets: (i) *Breast Cancer Wisconsin (Diagnostic)* Blake (1998) which classifies malignant/benign tumors; (ii) *Student Performance* Cortez and Silva (2008) which predicts the student grade with survey questionnaires; and (iii) *Titanic* Kaggle (2018) which predicts if passengers survived the Titanic shipwreck.

Evaluation Metrics. For each input x , CF explanation techniques (including CounterNet) generate two outputs: (i) a prediction \hat{y}_x ; and (ii) a CF example x' , which receives a different prediction $\hat{y}_{x'}$ (for binary classification problems, $\hat{y}_x + \hat{y}_{x'} = 1$). We evaluate the quality of both these outputs using separate metrics. For evaluating predictions, we use *predictive accuracy* (as all six datasets are fairly class-balanced). For evaluating CF explanations, we use three separate metrics: (i) *Validity*, is defined as the fraction of input instances on which CF explanation techniques output valid CF explanations, i.e., $\hat{y}_x + \hat{y}_{x'} = 1$. (ii) *Proximity*, is defined as the L_1 norm distance between the input x and the generated CF x' . (iii) Finally, we propose a novel metric, called *Insensitivity Score*, which measures the robustness of the generated CF example against small manipulations. Formally, let $x = \{x_1, x_2, \dots, x_d\}$ and $x' = \{x'_1, x'_2, \dots, x'_d\}$ be the features of the input data point and the CF example, respectively. To measure the *insensitivity score* of CF x' , we use a threshold of b , and create a new data point $x'' = \{l_i = \mathbb{1}_{|x_i - x'_i| \leq b} x_i + \mathbb{1}_{|x_i - x'_i| > b} x'_i \forall i \in 1 \dots d\}$, i.e., we replace all features $i \in \{1, d\}$ in x' for which $|x_i - x'_i| \leq b$. Intuitively, x'' represents a slightly altered version of our CF example x' in which we neglect feature differences less than b . We repeat this procedure for every input instance and its corresponding CF example. Finally, *insensitivity score* is defined as the fraction of input data points x on which x'' also remains a valid CF example.

Rationale of Metrics. High *predictive accuracy* is vital as we do not want to provide explanations for incorrect predictions made by an ML model. For the quality of CF examples, (i) high *validity* implies the technique’s effectiveness at creating valid CF examples; (ii) high *proximity* implies fewer modifications that need to be made in the input space to convert it into a valid CF example; and finally (iii) high *insensitivity score* is desirable for any CF explanation technique. Intuitively, techniques with high insensitivity enable us to create end-user explanations based on only features in x which differ significantly from corresponding feature values in x' while completely neglecting small feature differences (less than b). This refers to the modified counterfactual example x'' (which neglects small feature differences between x and x') remaining as a valid counterfactual. Thus, high insensitivity aids interpretability from an end-user perspective.

5 Evaluating CounterNet Performance

In short, Tables 1 and 2 show that CounterNet achieves superior performance over baseline CF explanation techniques. First, CounterNet can consistently generate CF examples with more than 98% validity (whereas baseline methods perform poorly on specific datasets). In particular, VanillaCF uses a post-hoc CF generation method similar to CounterNet; yet, it achieves 17% lower validity on datasets with large number of categorical features. This illustrates the misalignment between the objectives of predictive model training and CF explanation inside post-hoc methods like VanillaCF. Second, CF examples generated by CounterNet are

Table 2: Evaluation of Counterfactual Examples

Datasets	Metrics	Methods				
		VanillaCF	DiverseCF	ProtoCF	VAE-CF	CounterNet
Adult	Validity	0.758	0.535	0.589	0.664	0.994
	Proximity	5.804	8.002	7.169	8.627	7.156
	Insensitivity	1.000	0.997	0.996	0.994	1.000
	Running time	1821.737	6307.111	2492.588	3.037	0.915
HELOC	Validity	1.000	0.904	0.998	1.000	0.986
	Proximity	5.403	5.230	5.879	7.727	4.389
	Insensitivity	1.000	0.992	1.000	1.000	1.000
	Running time	1572.875	4836.099	2508.052	2.682	0.655
OULAD	Validity	1.000	0.687	1.000	1.000	0.995
	Proximity	12.842	14.821	13.644	14.576	11.923
	Insensitivity	1.000	0.923	1.000	1.000	0.996
	Running time	2138.736	7110.721	2570.173	3.119	1.101
Student	Validity	0.803	0.527	0.325	0.491	0.987
	Proximity	13.213	18.909	16.305	21.413	20.109
	Insensitivity	0.990	0.987	0.987	0.993	1.000
	Running time	2558.077	9176.334	2609.500	3.650	1.657
Titanic	Validity	0.977	0.524	0.762	0.376	0.991
	Proximity	16.259	18.137	16.458	19.661	15.02
	Insensitivity	N.A.	1.000	N.A.	1.000	1.000
	Running time	3213.318	1250.652	2478.933	4.188	2.282
Breast Cancer	Validity	1.000	1.000	1.000	1.000	1.000
	Proximity	1.422	1.007	0.729	1.410	1.507
	Insensitivity	0.699	0.195	0.294	0.216	0.944
	Running time	1270.284	4058.734	2415.588	2.444	0.537

highly proximal — CounterNet outperforms baseline methods in half of the datasets and remains competitive in other datasets. Third, the high validity of CounterNet’s CF examples does not come at a cost of lowered predictive accuracy. In fact, CounterNet’s predictor network is only 0.5% less accurate than the base predictive model (averaged across six datasets) which is solely optimized for predictive accuracy. Finally, CounterNet runs in a fraction of time taken by its competitors - it is 3X faster than its nearest competitor and is orders of magnitude faster than the remaining baselines.

Counterfactual Validity. Table 2 compares the validity of CF examples generated by CounterNet and other baselines on all six datasets. This table shows that CounterNet achieves over 98% validity on all six datasets. In particular, CounterNet achieves $\sim 30\%$, $\sim 20\%$, $\sim 2\%$ higher validity than VanillaCF (its closest competitor) on the Adult, Student, and Titanic datasets, respectively. On the other hand, the performance of CounterNet (and other baselines) is fairly saturated on the HELOC, OULAD and Breast Cancer datasets. CounterNet achieves an average validity of $\sim 99\%$ on these three datasets, whereas VanillaCF achieves a validity of 100%.

Note that the first three datasets (Adult, Student and Titanic) have disproportionately more categorical features than continuous features, whereas the last three datasets (HELOC, OULAD and Breast Cancer) are opposite (see Table 1). Thus, the results in Table 2 illustrate two things: (i) CounterNet consistently achieves more than 98% validity on all six datasets; (ii) while baseline methods achieve high validity on datasets which contain disproportionate number of continuous features, they achieve poor validity on the first three datasets (e.g.,

Table 3: Evaluation of CounterNet’s Predictive Accuracy

Dataset	Base Model	CounterNet
Adult	0.831	0.828
Student	0.908	0.920
Titanic	0.816	0.821
HELOC	0.717	0.716
OULAD	0.934	0.929
Breast Cancer	0.972	0.958

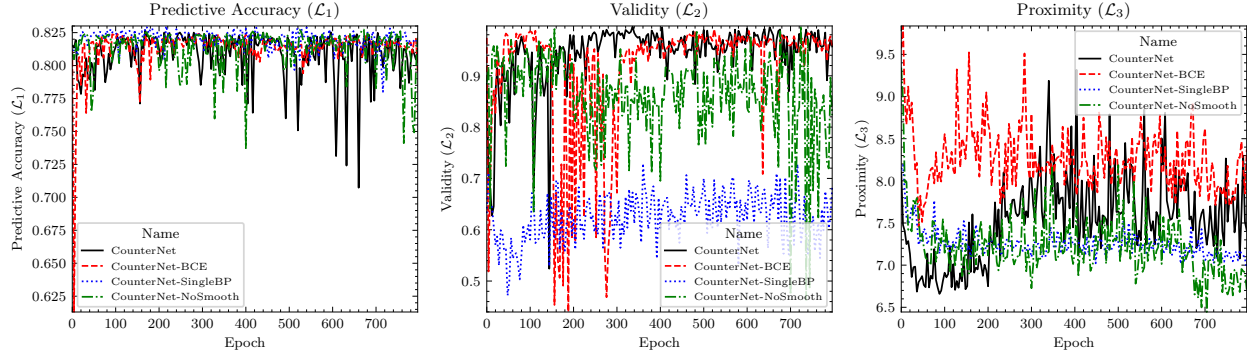


Figure 2: Learning curves of \mathcal{L}_1 , \mathcal{L}_2 , and \mathcal{L}_3 of model ablations on the Adult dataset.

CounterNet outperforms the best performing baseline by 17% on these datasets). These results highlight the difficulty of achieving high validity with categorical features, and shows that baseline methods are ill-suited for these tasks.

Counterfactual Proximity & Insensitivity Score. Table 2 compares the proximity/insensitivity score achieved by CounterNet and baselines on all six datasets. CounterNet is highly proximal (i.e. the L_1 norm distance between the input instance and the CF example is small) against the baseline methods. In particular, CounterNet achieves the highest proximity on the HELOC, OULAD, and Titanic. In all other datasets, CounterNet performs as well as other baselines, as it matches the average proximity value in other baselines. These results further illustrate CounterNet’s advantages on generating highly aligned and interpretable CF explanations.

In terms of the insensitivity, we use a fixed threshold $b = 2$ to compute the insensitivity score. Table 2 shows that on the Breast Cancer dataset, CounterNet achieves $\sim 40\%$ higher insensitivity score as compared to VanillaCF (the closest competitor). On all other datasets, all methods achieve comparable insensitivity score, e.g., CounterNet achieves 100% insensitivity score on the Adult, HELOC, Student, and Titanic datasets. On the Titanic dataset, VanillaCF and ProtoCF have N.A. values, as they did not generate any CF examples with feature differences less than $b = 2$.

Predictive Accuracy. Table 1 compares the predictive accuracy achieved by CounterNet against the base prediction model used by our baseline methods. This table shows that CounterNet exhibits highly competitive performance in terms of predictive accuracy on all six datasets. CounterNet achieves marginally better accuracy on the Student, Titanic and HELOC datasets (row 2,3 & 4), and achieves marginally lower accuracy on the remaining datasets. Across all six datasets, the difference between the predictive accuracy of CounterNet and the base model is $\sim 0.5\%$. This table illustrates that potential benefits achieved by CounterNet’s joint training of predictor and CF generator networks do not come at a cost in terms of reduced predictive accuracy.

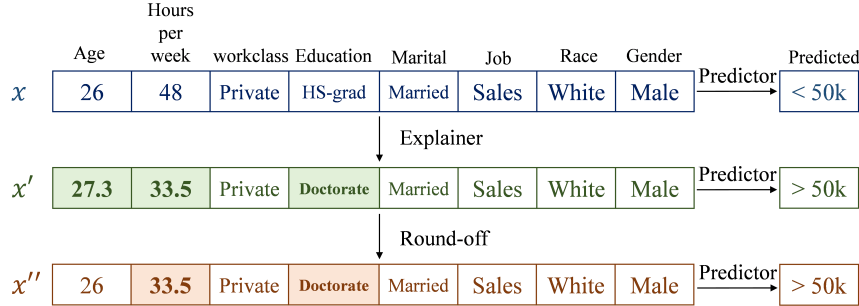


Figure 3: A counterfactual explanation generated by CounterNet.

Runtime Comparison. Table 2 shows the average runtime (in milliseconds) taken by CounterNet and other baselines in generating a CF example for a single data point in the test data. The result highlights that CounterNet generates CF examples $\sim 3X$ (on average) faster than VAE-CF (the closest competitor). Moreover, CounterNet runs three orders of magnitude faster than the other baselines, out of which DiverseCF runs slowest, followed by ProtoCF and VanillaCF (with average runtime across six datasets of 4592, 2328, and 1576 ms, respectively). This result shows CounterNet’s ability to be adopted in time-constrained environments.

Ablation Analysis. We analyze the importance of design choices inside CounterNet on the resulting interpretability/predictive accuracy. We analyze three ablations of CounterNet, each of which is created by replacing a specific model component in CounterNet with an alternate choice. First, we highlight the importance of the MSE loss functions used to optimize the CounterNet network (Eq. 1) by replacing the MSE based \mathcal{L}_1 and \mathcal{L}_2 loss in Eq. 1 with cross entropy loss (*CounterNet-BCE*). Second, we highlight the importance of CounterNet’s novel double-back BP procedure by using conventional one-pass-through backpropagation optimization to train CounterNet instead (*CounterNet-SingleBP*). Finally, we highlight the importance of label smoothing by excluding it from CounterNet (*CounterNet-NoSmooth*).

Figure 2 compares the individual learning curves for the \mathcal{L}_1 , \mathcal{L}_2 and \mathcal{L}_3 loss functions achieved by CounterNet and our three ablations on adult dataset. This figure shows that compared to the CounterNet’s learning curve for \mathcal{L}_2 , *CounterNet-BCE* and *CounterNet-NoSmooth*’s learning curves has significantly higher instability, illustrating the importance of MSE-based loss function and label smoothing techniques in CounterNet’s superior performance. Moreover, *CounterNet-SingleBP*’s learning curve for \mathcal{L}_2 performs poorly in comparison, which illustrates the difficulty of optimizing three divergent loss functions inside CounterNet using a single backpropagation procedure. In turn, this also illustrates the effectiveness of our double-back BP procedure in CounterNet’s training. These results show that all design choices made in Section 3 contribute to training the model effectively.

Real-World Usage. We now illustrate how CounterNet can generate interpretable explanations for end-users. Figure 3 shows an actual data point x from the Adult dataset, and the corresponding valid CF example x' generated by CounterNet. This figure shows that x and x' only differ in three features (Age, Hours/week, and Education). Instead of generating an explanation to the end-user in terms of all three features, CounterNet generates x'' by ignoring feature differences that are less than threshold $b = 2$ (in practice, domain experts can help identify realistic values of b). Note that due to CounterNet’s high levels of insensitivity, x'' also remains a valid CF example. After this post-processing step, x and x'' differ in exactly two features (Hours/week and Education), and the end-user is provided with the following natural-language explanation: “*If you want the ML model to predict that you will earn more than US\$50K, change your education from HS-Grad to Doctorate, and reduce the number of hours of work/week from 48 to 33.5.*”

6 Discussion & Conclusion

Although our experimental evaluation exhibits CounterNet’s superior performance (as compared to post-hoc baselines), these two methods have somewhat different motivations. While post-hoc methods are designed for use in situations when counterfactual explanations need to be generated for proprietary black-box ML models (whose training data and model parameters are not accessible), CounterNet is designed for situations when the training data is accessible to the counterfactual explanation system designers and hence it can be exploited to optimize the generation of CF examples. Nevertheless, CounterNet can be used to interpret proprietary ML models by forcing its predictor network to mimic that proprietary ML model (via supervised training).

CounterNet has two limitations. First, CounterNet does not consider other desirable aspects in CF explanations, such as diversity (Mothilal et al., 2020), recourse cost (Ustun et al., 2019), and causality (Karimi et al., 2021). Further research is needed to address these issues. Finally, although CounterNet is suitable for real-time deployment given its superior performance in validity and speed, one must be aware of the possible negative impacts to the end-users. It is important to ensure that generated CF examples do not amplify or provide support to the narratives resulting from pre-existing race-based and gender-based societal inequities (among others). One short-term workaround is to have human in the loop. We can provide CounterNet’s explanations as a decision-aid to a well-trained human official, who is in charge of communicating the decisions of ML models to human end-users in a respectful and humane manner. In the long-run, further studies are needed to understand the social impacts of CounterNet.

This paper proposes *CounterNet*, a novel learning framework which integrates predictive model training and CF example generation into a single *end-to-end* pipeline. Unlike prior work, CounterNet ensures that the objectives of predictive model training and CF example generation are closely aligned. We also propose a novel BP variant to remedy the difficulty of training CounterNet. Experimental analysis on six real-world datasets shows that CounterNet outperforms state-of-the-art baselines in validity, proximity, insensitivity, and runtime, and is highly competitive in predictive accuracy.

References

Agarwal, S. (2020). Trade-offs between fairness and interpretability in machine learning. *Proc. 3rd International Workshop on AI for Social Good*.

Bhatt, U., Xiang, A., Sharma, S., Weller, A., Taly, A., Jia, Y., Ghosh, J., Puri, R., Moura, J. M. F., and Eckersley, P. (2020). Explainable machine learning in deployment. In *Proceedings of the 2020 Conference on Fairness, Accountability, and Transparency*, FAT* ’20, page 648–657, New York, NY, USA. Association for Computing Machinery.

Binns, R., Van Kleek, M., Veale, M., Lyngs, U., Zhao, J., and Shadbolt, N. (2018). ‘it’s reducing a human being to a percentage’ perceptions of justice in algorithmic decisions. In *Proceedings of the 2018 CHI conference on human factors in computing systems*, pages 1–14.

Blake, C. (1998). Uci repository of machine learning databases. <http://www.ics.uci.edu/~mlearn/MLRepository.html>.

Caruana, R., Lou, Y., Gehrke, J., Koch, P., Sturm, M., and Elhadad, N. (2015). Intelligible models for healthcare: Predicting pneumonia risk and hospital 30-day readmission. In *Proceedings of the 21th ACM SIGKDD international conference on knowledge discovery and data mining*, pages 1721–1730.

Chen, C., Li, O., Tao, D., Barnett, A., Rudin, C., and Su, J. K. (2019). This looks like that: deep learning for interpretable image recognition. In *Advances in neural information processing systems*, pages 8930–8941.

Cortez, P. and Silva, A. M. G. (2008). Using data mining to predict secondary school student performance.

Dhurandhar, A., Chen, P.-Y., Luss, R., Tu, C.-C., Ting, P., Shanmugam, K., and Das, P. (2018). Explanations based on the missing: Towards contrastive explanations with pertinent negatives. In *Proceedings of the 32nd International Conference on Neural Information Processing Systems*, NIPS’18, page 590–601, Red Hook, NY, USA. Curran Associates Inc.

FICO (2018). Explainable machine learning challenge. <https://community.fico.com/s/explainable-machine-learning-challenge>.

He, K., Zhang, X., Ren, S., and Sun, J. (2016). Deep residual learning for image recognition. In *Proceedings of the IEEE conference on computer vision and pattern recognition*, pages 770–778.

Kaggle (2018). Titanic - machine learning from disaster. <https://www.kaggle.com/c/titanic/overview>.

Karimi, A.-H., Schölkopf, B., and Valera, I. (2021). Algorithmic recourse: from counterfactual explanations to interventions. In *Proceedings of the 2021 ACM Conference on Fairness, Accountability, and Transparency*, pages 353–362.

Kohavi, R. and Becker, B. (1996). Uci machine learning repository: Adult data set.

Kuzilek, J., Hlosta, M., and Zdrahal, Z. (2017). Open university learning analytics dataset. *Scientific data*, 4:170171.

Lakkaraju, H., Bach, S. H., and Leskovec, J. (2016). Interpretable decision sets: A joint framework for description and prediction. In *Proceedings of the 22nd ACM SIGKDD international conference on knowledge discovery and data mining*, pages 1675–1684.

Lou, Y., Caruana, R., Gehrke, J., and Hooker, G. (2013). Accurate intelligible models with pairwise interactions. In *Proceedings of the 19th ACM SIGKDD international conference on Knowledge discovery and data mining*, pages 623–631.

Lundberg, S. M. and Lee, S.-I. (2017). A unified approach to interpreting model predictions. In *Advances in neural information processing systems*, pages 4765–4774.

Mahajan, D., Tan, C., and Sharma, A. (2019). Preserving causal constraints in counterfactual explanations for machine learning classifiers. *arXiv preprint arXiv:1912.03277*.

Mothilal, R. K., Sharma, A., and Tan, C. (2020). Explaining machine learning classifiers through diverse counterfactual explanations. In *Proceedings of the 2020 Conference on Fairness, Accountability, and Transparency*, pages 607–617.

Müller, R., Kornblith, S., and Hinton, G. (2019). When does label smoothing help? *arXiv preprint arXiv:1906.02629*.

Pawelczyk, M., Broelemann, K., and Kasneci, G. (2020). Learning model-agnostic counterfactual explanations for tabular data. In *Proceedings of The Web Conference 2020*, pages 3126–3132.

Ribeiro, M. T., Singh, S., and Guestrin, C. (2016). ” why should i trust you?” explaining the predictions of any classifier. In *Proceedings of the 22nd ACM SIGKDD international conference on knowledge discovery and data mining*, pages 1135–1144.

Rudin, C. (2019). Stop explaining black box machine learning models for high stakes decisions and use interpretable models instead. *Nature Machine Intelligence*, 1(5):206–215.

Salimans, T., Goodfellow, I., Zaremba, W., Cheung, V., Radford, A., and Chen, X. (2016). Improved techniques for training gans. *arXiv preprint arXiv:1606.03498*.

Sharma, S., Henderson, J., and Ghosh, J. (2020). Certifai: A common framework to provide explanations and analyse the fairness and robustness of black-box models. In *Proceedings of the AAAI/ACM Conference on AI, Ethics, and Society*, AIES ’20, page 166–172, New York, NY, USA. Association for Computing Machinery.

Srivastava, N., Hinton, G., Krizhevsky, A., Sutskever, I., and Salakhutdinov, R. (2014). Dropout: a simple way to prevent neural networks from overfitting. *The journal of machine learning research*, 15(1):1929–1958.

Ustun, B., Spangher, A., and Liu, Y. (2019). Actionable recourse in linear classification. In *Proceedings of the Conference on Fairness, Accountability, and Transparency*, pages 10–19.

Van Looveren, A. and Klaise, J. (2019). Interpretable counterfactual explanations guided by prototypes. *arXiv preprint arXiv:1907.02584*.

Verma, S., Dickerson, J., and Hines, K. (2020). Counterfactual explanations for machine learning: A review. *arXiv preprint arXiv:2010.10596*.

Wachter, S., Mittelstadt, B., and Russell, C. (2017). Counterfactual explanations without opening the black box: Automated decisions and the gdpr. *Harv. JL & Tech.*, 31:841.

Xu, B., Wang, N., Chen, T., and Li, M. (2015). Empirical evaluation of rectified activations in convolutional network. *arXiv preprint arXiv:1505.00853*.

A Proof of Lemma 3.1

Proof. $\nabla_{\theta}\mathcal{L}_1 = \nabla_{\theta} \|y_i - \hat{y}_{x_i}\|^2$, and $\nabla_{\theta}\mathcal{L}_2 = \nabla_{\theta} \left\| y_i - (1 - \hat{y}_{x'_i}) \right\|^2$. We have

$$\nabla_{\theta}\mathcal{L}_1 = \begin{cases} \nabla_{\theta}\hat{y}_{x_i}^2 & , \text{if } y_i = 0 \\ \nabla_{\theta}(1 - \hat{y}_{x_i})^2 & , \text{if } y_i = 1 \end{cases}$$

$$\nabla_{\theta}\mathcal{L}_2 = \begin{cases} \nabla_{\theta}(1 - \hat{y}_{x'_i})^2 & , \text{if } y_i = 0 \\ \nabla_{\theta}\hat{y}_{x'_i}^2 & , \text{if } y_i = 1 \end{cases}$$

Since $x'_i \rightarrow x_i$ as we expect CF example x'_i is closed to the original instance x_i , we can replace x'_i to x_i in \mathcal{L}_2 . Then, we have

$$\nabla_{\theta}\mathcal{L}_2 = \begin{cases} \nabla_{\theta}(1 - \hat{y}_{x_i})^2 & , \text{if } y_i = 0 \\ \nabla_{\theta}\hat{y}_{x_i}^2 & , \text{if } y_i = 1 \end{cases}$$

Therefore,

$$\begin{aligned} \nabla_{\theta}\mathcal{L}_1 \cdot \nabla_{\theta}\mathcal{L}_2 &= \nabla_{\theta}(1 - \hat{y}_{x_i})^2 \cdot \nabla_{\theta}\hat{y}_{x_i}^2 \\ &= 2(1 - \hat{y}_{x_i}) \cdot (-\nabla_{\theta}\hat{y}_{x_i}) \cdot 2(\hat{y}_{x_i}) \cdot \nabla_{\theta}\hat{y}_{x_i} \\ &= 2(1 - \hat{y}_{x_i}) \cdot 2\hat{y}_{x_i} \cdot -(\nabla_{\theta}\hat{y}_{x_i})^2 \end{aligned}$$

where $1 - \hat{y}_{x_i} > 0$, $\hat{y}_{x_i} > 0$, and $(\nabla_{\theta}\hat{y}_{x_i})^2 > 0$. Therefore, $\nabla_{\theta}\mathcal{L}_1 \cdot \nabla_{\theta}\mathcal{L}_2 < 0$.

□

B Implementation Details

Here we provide implementation details of CounterNet and four baselines on six datasets listed in Section 5. The code can be found through this GitHub repository: <https://github.com/BirkhoffG/counternet>.

B.1 Software and Hardware Specification

We use Python (v3.7) with Pytorch (v1.60), Pytorch Lightning (v1.10), numpy (v1.19.3), pandas (1.1.1) and scikit-learn (0.23.2) for the implementations. All our experiments were run on a Debian-10 Linux-based Deep Learning Image with CUDA 11.0 on the Google Cloud Platform.

The CounterNet' network is trained on NVIDIA Tesla V100 with an 8-core Intel machine. CF generation of four baselines are run on a 16-core Intel machine with 64 GB of RAM. The evaluation (results in Table 1 & 2 in the paper) are generated from the same 16-core machine.

B.2 CounterNet Implementation Details

Across all six datasets, we apply the following same settings in training CounterNet: We initialize the weights as in He et al. (2016). We adopt the Adam with mini-batch size of 128. For each datasets, we trained the models for up to 1×10^3 iterations. To avoid gradient explosion, we apply gradient clipping by setting the threshold to 0.5 to clip gradients with norm above 0.5. We set dropout rate to 0.3 to prevent overfitting. For all six datasets, we set $\lambda_1 = 1.0$, $\lambda_2 = 0.2$, $\lambda_3 = 0.01$ in Equation 2.

The learning rate is the only hyper-parameter that varies across six datasets. From our empirical study, we find the training to CounterNet is sensitive to the learning rate, although a good choice of loss function (e.g. choosing MSE over cross-entropy) can widen the range of an "optimal" learning rate. We apply grid search to tune the learning rate, and our choice is specified in Table 4.

Additionally, we specify the architecture's details (e.g. dimensions of each layer in encoder, predictor and CF generator) in Table 4. The numbers in each bracket represent the dimension of the transformed matrix. For example, the encoder dimensions for adult dataset is [29, 50, 10], which means that the dimension of input $x \in \mathbb{R}^d$ is 29 (e.g. $d = 29$); the encoder first transforms the input into a 50 dimension matrix, and then downsamples it to generate the latent representation $z \in \mathbb{R}^k$ where $k = 10$.

Dataset	Learning Rate	Encoder Dims	Predictor Dims	CF Generator Dims
Adult	0.01	[29, 50, 10]	[10, 10, 2]	[20, 50, 29]
HELOC	0.005	[35, 100, 10]	[10, 10, 2]	[20, 100, 35]
OULAD	0.001	[127, 200, 10]	[10, 10, 2]	[20, 200, 127]
Student	0.01	[85, 100, 10]	[10, 10, 2]	[20, 100, 85]
Titanic	0.01	[57, 100, 10]	[10, 10, 2]	[20, 100, 57]
Breast Cancer	0.001	[30, 50, 10]	[10, 10, 2]	[20, 50, 30]

Table 4: Hyperparameters and architectures for each dataset.

B.3 Hyper-parameters for Baselines

Next, we describe the implementation of baseline methods. For VanillaCF and ProtoCF, we follow author's instruction as much as we can, and implement them in Pytorch. For VanillaCF, DiverseCF and ProtoCF, we run maximum 1×10^3 steps. After CF generation, we convert the results to one-hot-encoding format for each categorical feature. For training the VAE-CF, we follow Mahajan et al. (2019)'s settings on running maximum 50 epoches and setting the batch size to 1024. We use the same learning rate as in Table 4 for VAE training.

For training predictive models for baseline algorithms, we apply grid search for tuning the learning rate, which is specified in Table 5. Similar to training the CounterNet, we adopt the Adam with mini-batch size of 128, and set the dropout rate to 0.3. We train the model for up to 100 iterations with early stopping to avoid overfittings.

Dataset	Learning Rate
Adult	0.01
HELOC	0.005
OULAD	0.001
Student	0.01
Titanic	0.01
Breast Cancer	0.001

Table 5: Learning rate of the base predictive models on each dataset

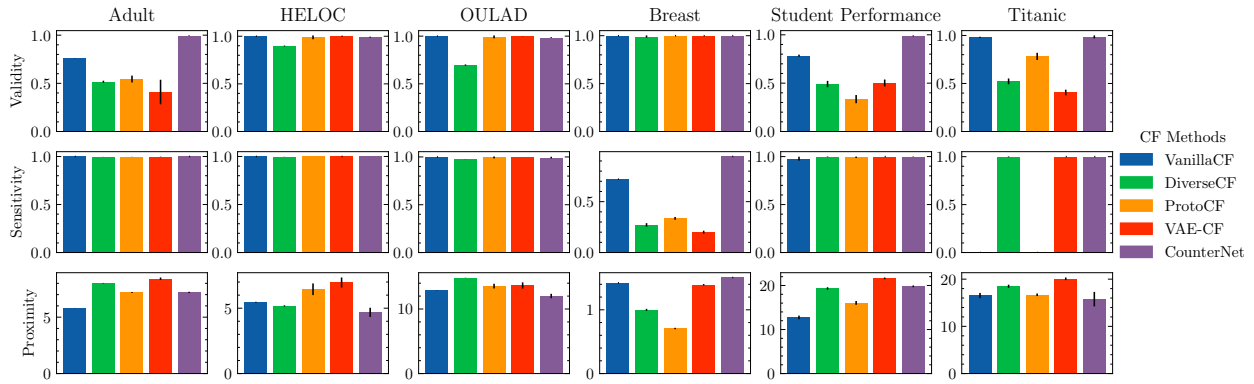


Figure 4: Plots on the evaluation of counterfactual explanations with error bar.

C Additional Experimental Results

C.1 Impact of Neural Network Structures

We further study the impact of the different neural network blocks. In our experiment, we primarily use multi-layer perception as it is a suitable baseline model for the tabular data. For comparison, We also implemented the CounterNet with Convolutional building blocks (i.e. replace the feed forward neural network with convolution layer). We implemented the convolutional CounterNet on the Adult dataset. To train the feed forward neural network with convolution layers, we set the learning rate as 0.03 and $\lambda_1 = 1.0$, $\lambda_2 = 0.4$, $\lambda_3 = 0.01$. The rest configuration is exactly the same as training CounterNet with MLP.

Table 6 shows comparision between for the CounterNet with convolutional building blocks (*CounterNet-Conv*) and multi-layer perceptions (*CounterNet-MLP*). The results indicate that CounterNet-Conv matches the performances of CounterNet-MLP. CounterNet-Conv performs slightly worse than CounterNet-MLP because convolutional layer is not suitable for tabular datasets. Yet, CounterNet-Conv outperforms the rest of baselines in validity and insensitivity (with reasonably good proximity score). This illustrates CounterNet’s potential real-world usage in various settings as it is agnostic to the network structures.

Building Block	Predictive Accuracy	Validity	Proximity	Insensitivity
CounterNet-Conv	0.823	0.980	7.554	1.000
CounterNet-MLP	0.828	0.994	7.156	1.000

Table 6: Results for the CounterNet with Convolution layers on Adult dataset.

C.2 Supplemental Results for CF Techniques

Figure 4 contains the results of CF explanations generated by baseline methods and CounterNet. This figure’s result is the same as Table 2 in the paper, except it contains results with error bar. Figure 4 further corroborates our findings that CounterNet consistently outperforms the state-of-the-art baselines.

C.3 Additional Ablation Analysis

We provide supplementary results on ablation analysis of other two large datasets (HELOC and OULAD, shown in Figure 5 & 6, respectively). We observe the similar pattern as Figure 2 in the original paper.

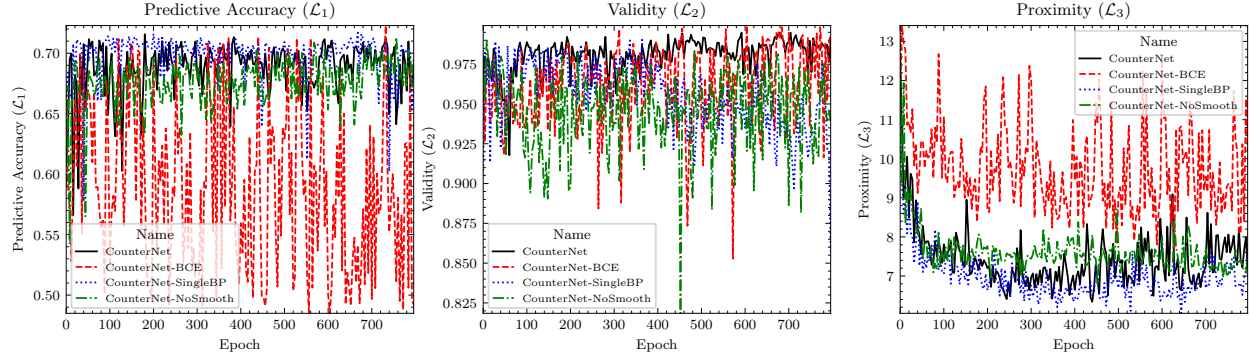


Figure 5: Learning curves of \mathcal{L}_1 (left), \mathcal{L}_2 (mid), and \mathcal{L}_3 (right) of model ablations on the HELOC dataset.

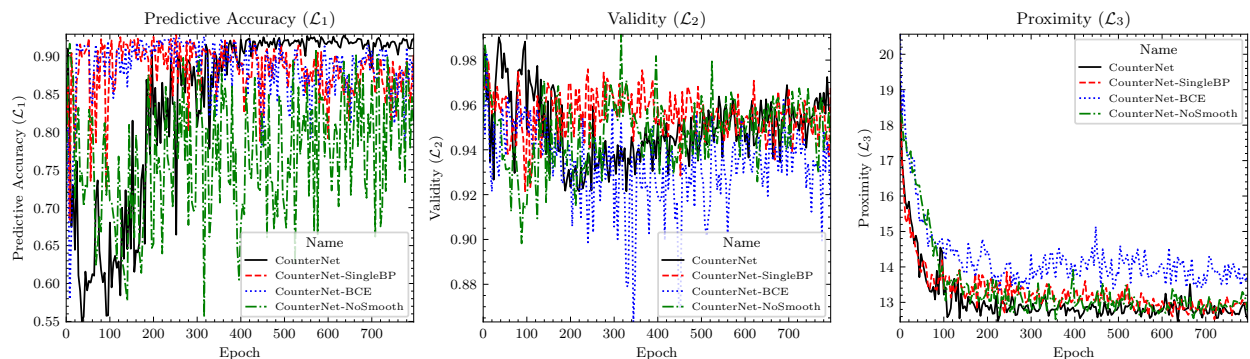


Figure 6: Learning curves of \mathcal{L}_1 (left), \mathcal{L}_2 (mid), and \mathcal{L}_3 (right) of model ablations on the OULAD dataset.